

# Techno feasibility analysis of a concentrating solar thermal cooling systems at a university complex

Lucas de Oliveira Alves <sup>a</sup>, Diego Cunha Malagueta <sup>b</sup> & Elisa Pinto da Rocha <sup>b</sup>

<sup>a</sup> Programa de Planejamento Energético, COPPE, Universidade Federal do Rio de Janeiro, Brasil. lucasoa@ppe.ufrj.br

<sup>b</sup> Engenharia Mecânica, Campus Macaé, Universidade Federal do Rio de Janeiro, Brasil. diegom@ppe.ufrj.br, elisarocha@macae.ufrj.br

Received: January 25<sup>th</sup>, 2021. Received in revised form: April 20<sup>th</sup>, 2021. Accepted: May 3<sup>rd</sup>, 2021.

## Abstract

Concentrating solar thermal (CST) energy applications are growing worldwide, especially in combined cooling, heat, and power processes. Building upon the analysis of a building's thermal comfort, and software simulations for CST, the current study evaluates a solar conditioning system integrated with absorption systems. The cooling system is equipped with single-, double- and triple-effect configurations cycle, production parameters, and thermal storage. The required fraction of auxiliary energy for the system operation is estimated. The results indicate that the double effect system is the best configuration for the adopted location in Brazil. The system's annual auxiliary energy demand is, approximately, 20%. Triple-effect systems require less energy at higher temperatures due to local direct radiation, which then leads to an intermittent operation and greater auxiliary energy demands. The methodology applied in this work could be adopted in different locations, with an emphasis on the possibility of testing smaller scale systems in small buildings.

*Keywords:* concentrating solar energy; absorption refrigeration; simulation.

# Análisis de viabilidad técnica de un sistema de refrigeración termosolar por concentración en un complejo universitario

## Resumen

Las aplicaciones de la energía solar térmica de concentración (CST) están creciendo en todo el mundo, especialmente en los procesos combinados de refrigeración, calor y electricidad. Partiendo del análisis del confort térmico de un edificio y de simulaciones de software para CST, el presente estudio evalúa un sistema de acondicionamiento solar integrado con sistemas de absorción. El sistema de refrigeración está equipado con configuraciones de ciclo de efecto simple, doble y triple, parámetros de producción y almacenamiento térmico. Se estima la fracción de energía auxiliar necesaria para el funcionamiento del sistema. Los resultados indican que el sistema de doble efecto es la mejor configuración para la ubicación adoptada en Brasil. La demanda anual de energía auxiliar del sistema es, aproximadamente, del 20%. Los sistemas de triple efecto requieren menos energía a temperaturas más altas debido a la radiación directa local, lo que lleva a un funcionamiento intermitente y a una mayor demanda de energía auxiliar. La metodología aplicada en este trabajo podría adoptarse en diferentes lugares, haciendo hincapié en la posibilidad de probar sistemas de menor escala en edificios pequeños.

*Palabras clave:* concentración de energía solar; refrigeración por absorción; simulación.

## 1. Introduction

Solar energy is one of the most promising sources of power in the face of the energy challenges of the millennium. The technology has wide applications in thermal, dynamic, or chemical processes [1]. For example, water heating [2], air conditioning [3], electric power generation [4,5], and cogeneration systems [6,7].

The world has been experiencing a significant increase in electrical demand associated with more frequent use of air conditioners, which are responsible for about 20% of all electricity used in buildings worldwide [8]. Current estimates predict a growing household demand for air conditioners, from 1.6 billion air conditioners in 2018 to 5.6 billion units by 2050 [8]. This growth in air conditioning technologies to

**How to cite:** Alves, L. de O., Malagueta, D.C. and da Rocha, E., Techno feasibility analysis of a concentrating solar thermal cooling systems at a university complex.. DYNA, 88(217), pp. 282-291, April - June, 2021.

generate cooling services has a direct impact on the emissions of CO<sub>2</sub> to the atmosphere as many electrical generation systems still rely on fossil fuels burning for operation.

Looking into a nationwide example and metrics to analyze the effects of air conditioning and CO<sub>2</sub> emissions, Brazil is a good location for case studies. Although most of the country's electricity comes from hydroelectric power plants, there are several thermoelectric plants producing around 26.21% of all electricity used in the country [9], which increases CO<sub>2</sub> emissions, the main precursor to the greenhouse effect. The effect is that an increase in global temperatures will also drive up the energy demand for cooling systems [10]. Such effect was experienced in 2018 when higher temperatures in several parts of the world contributed to a respective 5% growth in energy consumption compared to the previous year [11].

The environmental impacts as well as the catastrophic consequences caused by the increase of CO<sub>2</sub> emissions need to be considered. Thence, investments in clean and sustainable technologies need to be implemented to mitigate the negative effects of technological options used to meet human comfort.

Based on the importance of the technologic development in renewable energies, this paper aimed to conduct a feasibility study for the dimensioning of an air conditioning system operated by a concentrating solar thermal (CST) plant in the installations of a University Complex located in the city of Macaé-RJ, Brazil. As a specific objective, this work investigated the best absorption system configuration (single-, double-, or triple-effect) for parabolic troughs with different optical efficiencies installed in the same place.

## 2. Absorption refrigeration systems using solar energy

### 2.1 Solar energy concentrator collectors

Direct radiation, which is the portion of the sun's radiation that does not suffer scattering in the atmosphere, is the most important parameter for the high efficiency obtained in solar concentrator collectors [12]. In Brazil, the northeastern region has the best radiation values, an average of approximately 6.0 Wh/m<sup>2</sup> [13], due to the semi-arid climate, and the lowest average cloud cover levels [14]. Specific areas such as the Midwest and west portions of Paraíba and Rio Grande do Norte states present good values of Direct Irradiation. These locations, therefore, have the greatest potential for the installation of concentrating solar plants. Solar concentrator collectors are used to supplying thermal energy at high temperatures. The technology for concentrator options includes parabolic cylindrical, linear Fresnel reflector, parabolic disk, and central tower [12].

Parabolic cylinder solar collectors, or parabolic trough collectors, consist of a concave mirror of parabolic shape that focuses the sun's rays onto a receiver containing a thermal fluid that transfers the absorbed heat to another fluid contained in a closed cycle. The fluid properties incorporate high thermal conductivity, thermal stability, and high specific heat. This fluid can be an oil, pressurized water, molten salts, among others.

The geometry and composition of the parabolic trough is a fundamental factor associated the technology efficiency. The four main parameters influencing the concentrator

efficiency are the parabola trough length, aperture width (distance between two rims), focal length, and rim angle (angle between the optical axis and the line connecting the mirror edge with the focal point) [15].

Sun tracking systems are often considered to improve the direct solar radiation levels striking the parabolic trough. A solar tracker allows the system to rotate according to the solar position during the day. The axis orientation most used for the technology is North-South alignment with East-West tracking [15].

### 2.2 Absorption cooling systems

Solar energy can be harnessed for applications in air conditioning systems through an absorption chiller. Absorption refrigeration (or cooling) systems are operated by thermal energy, either in cogeneration systems or from renewable sources [16], commonly in combined cycles from gas turbines, diesel engines [17], or solar plants [7]. Applications with the latter are motivated by policies to combat global climate change.

Unlike the steam compression system, which is considered a cycle operated by work, the absorption cycle is operated by thermal energy. Whereas the vapor compression refrigeration system uses a compressor work to increase the refrigerant fluid pressure and aid its circulation in a closed cycle; the absorption system uses a heat source for the vaporization of the refrigerant dissolved in an absorbent fluid [16]. In this process, water - lithium bromide (H<sub>2</sub>O-LiBr) and water-ammonia (H<sub>2</sub>O-NH<sub>3</sub>) are commonly used pairs of cooling systems [17].

Another parameter is the COP (Coefficient of Performance) of the absorption cycle. The COP measures the ratio between cooling energy (desired effect) to the thermal power of the generator (required energy). This parameter is highly relevant to verify whether local conditions allow the construction of an absorption plant using concentrated solar energy.

#### 2.2.1 Double and triple effect absorption systems

Due to the low COP offered by the single-effect cycles, systems with higher performances were developed. Generally, double and triple effect systems produce higher COP values when compared to simple single-effect systems. Part of the heat rejected in the condenser is recovered in the double and triple effect systems. Studies show that triple effect systems can reach COP values up to 1.2 [3,19].

For systems containing aqueous LiBr solution, studies demonstrate that an increase in the generator's operating temperature also elevates the performance of the system. However, this process can facilitate the crystallization of the solution as the increase in the generator temperature leads to higher LiBr concentrations in the solution [20].

## 3. Methodology

Building upon previous studies addressing absorption cooling systems, thermo-energetic simulations in buildings, and concentrating solar thermal (CST) systems, the current study conducts computer modeling merging the application of these technologies for empirical application at a university complex in Brazil.

SAM software (System Advisor Model, version 2018.11.11) is used to perform the computer simulations and support the feasibility analysis [21]. For the simulations, the study considered the combination of a cylindrical parabolic solar collector integrated with an absorption refrigeration unit. It is noteworthy that the system is equipped with a subsystem for the storage of thermal energy, as well as an auxiliary energy source that supplies electricity to the system in times when solar thermal energy is not available. The auxiliary energy is commonly used to stabilize the energy production and is fundamental in systems installed in medium radiation sites, which is the case for the University Campus in Macaé (UFRJ – Macaé campus). The auxiliary heat is produced by fossil fuel combustion systems (natural gas, LPG, diesel oil, among others) or biomass burning.

The optical efficiencies considered in the simulations were based on a geometric analysis, similar to [24] and applied by [22], to estimate the efficiency of a pilot concentrating solar power (CSP) plant built for low-cost technological development, located on the Federal University of Rio de Janeiro (UFRJ) campus in Macaé, as seen in Fig. 1 [23,24].

The developed parabolic trough is composed of the discretization of the parabolic curve in a set of flat mirrors. This discretization simplifies the manufacturing process as well as reduces the final costs of the project, nonetheless, the system will experience greater optical losses and a consequent reduction on efficiency.

Even though other technically and economically mature technologies can be applied for air conditioning using solar energy (e.g. a photovoltaic plant operating with an electric chiller), a pilot plant using parabolic cylinders collectors for an alternative solar air conditioning system in Macaé will contribute to scientific and technological learning. In addition, such system allows researchers to verify possible applications of the technology in regions characterized by medium quality direct solar resources, in contrast to well-known applications in sites with high direct solar radiation [25]. Therefore, three different absorption air cooling system configurations (single-, double-, and triple-effect) operated by solar thermal energy are proposed.

The methods detailed here perform both qualitative and quantitative analyses of the main variables used for computer

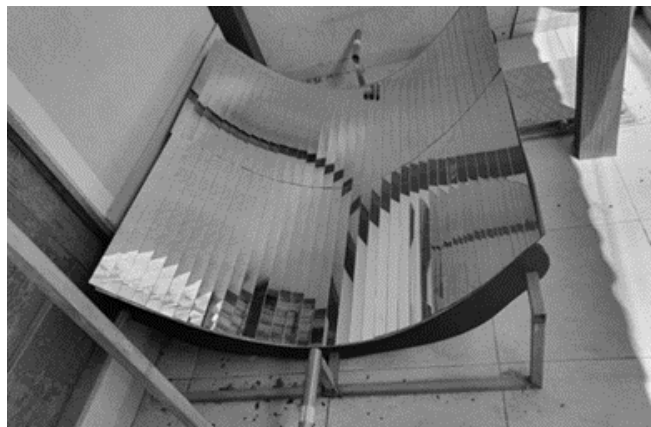


Figure 1. Parabolic trough mounted in the UFRJ- Macaé Campus. Source: the authors.

modeling. The first step was to obtain the thermal load profile required for cooling the university complex's ambient, described in section 3.1. Then, the peak thermal load, that will be required by the absorption cooling system evaporator, is obtained ( $Q_e$ ). The parameter is essential to finding the absorption cooling generator power ( $Q_g$ ), whose heat will be transferred from the CST system. The description of the absorption cooling system is presented in section 3.2. Section 3.3 details the methodology applied to obtain the thermal energy supplied by the solar system, which allows the study to evaluate the design variables and their influence on the global functioning of the conditioning system.

### 3.1. Conditioning thermal loads

Due to the complexity of the building design, with different types of rooms, a specific software can be essential to describe the thermal behavior for each ambient. The study adopted three software to analyze different components of the simulation. SketchUp 2017 was applied for 3-D modeling of the building, OpenStudio 2.8.0 was used to insert the boundary conditions, and EnergyPlus 8.7.0 performed calculations and generated results [26-30].

The 3-D modeling with SketchUp required the acquisition of the building external and internal characteristics, such as total building area, number and dimensions of rooms (floor, wall, and ceiling area), the number of windows and doors with their respective measures, positions, as well as the orientation of the building. These data were collected from the building floor plan and in loco visits.

The buildings have 3 floors. The first floor consists of administrative rooms, two toilets (men and women), and an auditorium. Classrooms and laboratories are located on the second and third floors, each floor contains two toilets. Rooms numbers go from 01 to 15, totaling 13 rooms per floor; rooms 01/02 and 04/05 shared spaces respectively, hereafter mentioned as “shared classrooms” (same logic for other shared spaces), while others simply “classrooms” (areas close to 60 to 70 m<sup>2</sup>).

The following step in the modeling is to characterize each thermal zone. The model requires data on climatic conditions, constructive characteristics, and appliance usage. These include: Climatic data for the city of Macaé; Physical properties of surface materials used internally and externally (walls, ceiling, and floor), as well as their coatings; Physical properties of sub-surface materials used internally and externally (windows and doors); Number of people per ambient, occupation profile, and type of activity; Lighting; Electrical equipment; Temperature required inside the environment; Infiltration.

OpenStudio allows users to introduce and change the building characteristics for the simulation. The results are important to analyze the impact of several variables on the model. For the simulation, rooms and the auditorium were divided into thermal zones based on their characteristics such as use, and internal heat gains profile. Hence, the 39 spaces (6 bathrooms, 1 auditorium, 4 shared classrooms, 22 classrooms, 5 administrative rooms, 1 shared administrative room) were grouped into 10 thermal zones. Table 1 shows each space and its respective thermal zone.

Table 1.  
Thermal zone and respective environment

Thermal Zone	Environment
Thermal Zone 1	Auditorium
Thermal Zone 2	Administrative room
Thermal Zone 3 and 4	Classrooms (2 <sup>nd</sup> and 3 <sup>rd</sup> floor)
Thermal Zone 5	Shared Classrooms (2nd floor)
Thermal Zone 6	Shared classrooms (3rd floor)
Thermal Zone 7, 8 and 9	Toilets (1 <sup>st</sup> , 2 <sup>nd</sup> and 3 <sup>rd</sup> floor)
Thermal Zone 10	Shared administrative room

Source: the authors.

### 3.2 Absorption refrigeration system

Three configurations are considered for the absorption cooling system: single-, double- and triple-effect. Each configuration requires different heat quantity and quality to operate. Usually, the greater the number of effects, the higher the heat temperature required by the cooling system. In addition, the COP is required to proceed with the simulation estimates. This parameter measures the relationship between the power of the evaporator ( $Q_e$ ), in the absorption refrigeration system, to the power required in the generator ( $Q_g$ ) served by the parabolic trough collector. The work required by the pump was considered negligible for the simulations.

The COP values were extracted from the scholarly literature [31]. For the single-effect configuration, the value of 0.65 [32] was adopted; for the double-effect, 1.36 [33]; and for the triple-effect, 1.80 [34]. Table 2 summarizes the COP values as well as the generator operating temperature ( $T_g$ ) adopted by each system configuration.

With regards to the system fluids, the study adopted lithium bromide (LiBr) and water (H<sub>2</sub>O) as a pair of working substances for the three stages. Water will act as a refrigerant and lithium bromide as an absorbent substance. This configuration is widely implemented for ambient air conditioning systems. According to Silva and Moreira [35], LiBr/H<sub>2</sub>O has numerous advantages for application in air conditioning systems such as high heat of vaporization, no need for rectification, it is non-hazardous to the environment.

### 3.3 Solar Technology simulations

The CST simulations were conducted right after the characterization of the absorption system. The System Advisor Model (SAM) software, version 2018.11.11 was used according by the following methodology.

For each absorption system configuration, 9 cases were modeled in the software. The cases were defined by combining the parabolic trough efficiency values,  $\eta = 0.5, 0.6,$  and  $0.7,$  and hours of thermal storage (TES),  $n = 6h, 8h$  and  $10h.$  The efficiency values adopted are within a range of

Table 2.  
Coefficient of performance values and Generator Temperature for each absorption cycle configuration

Absorption cycle	COP	Generator Temperature
Single-effect	0.65	80 °C
Double-effect	1.36	136 °C
Triple-effect	1.80	190 °C

Source: [30-32]

Table 3.  
Simulated cases regarding efficiency and storage time

Cases*	Efficiency	TES
LE/06	0.5	6h
LE/08	0.5	8h
LE/10	0.5	10h
ME/06	0.6	6h
ME/08	0.6	8h
ME/10	0.6	10h
HE/06	0.7	6h
HE/08	0.7	8h
HE/10	0.7	10h

\*: LE= low efficiency (0.5); ME= Medium efficiency (0.6); HE= High efficiency (0.7)

Source: the authors.

optical efficiencies from simplified concentrators up to values presented by commercial systems. For example, the efficiency of 0.5 was adopted as an approximation from the average values found in studies using a similar concentrating technology installed in the University Campus [22]. The highest efficiency (0.7) provides an estimate to the commercially produced concentrators around the world (efficiency around 0.8 to 0.85) [36]. Nevertheless, considering that panels manufactured domestically will show less efficiency, the cases were elaborated as shown in Table 3.

The subsequent step was to conduct a parametric (or sensitivity) analysis of the Solar Multiple (SM) in order to maximize the annual thermal energy production. The SM represents the ratio between the receiver's thermal power in the solar field and the heat sink power that will be delivered to the absorption system.

For each case, a parametric analysis was performed to determine the fluid outlet temperature that maximizes the annual energy production. For this, a set of values above the fluid inlet temperature was inserted, varying 5°C for each interval. It is worth mentioning that the fluid inlet temperature was obtained using an increase of  $\Delta T = 10^\circ C$  in relation to the generator temperature ( $T_g$ ); this procedure is widely adopted by literature [37-40]. Table 4 presents the values adopted as inlet fluid temperature for each absorption system arrangement.

Eq. 1 was used to estimate the heat sink's operating power:

$$COP = \frac{Q_e}{Q_g} \quad (1)$$

With the maximum thermal load for building conditioning obtained in section 'n' and the COP values adopted in Table 2, the heat sink thermal power ( $Q_g$ ) can be calculated.

Table 4.  
Inlet fluid temperature values for each absorption system arrangement

Absorption cycle	Inlet fluid temperature
Single-effect	90 °C
Double-effect	146 °C
Triple-effect	200 °C

Source: the authors.

Table 5.  
System Advisor Model (SAM) input variables

Software tab	Variables
System project	- direct normal irradiance (DNI)
	- Solar Multiple
	- solar field inlet fluid temperature
	- solar field outlet fluid temperature
	- thermal storage
Collector field	- Heat sink's thermal power
Collectors	- heat transfer fluid
	- collector chosen
Receptors	- optical parameters
	- receptor chosen

Source: the authors.

At the end of these parameterizations, all the parameter values necessary as input in the “system design” tab of the software is obtained. Table 5 summarizes the variables inserted in the program. The parameters related to the solar system were introduced in the following software tab. In this section, the thermal fluid chosen to perform the heat transfer was pressurized water, the other parameters were the system's default.

The commercial model SkyFuel SkyTrough collector was chosen for the simulations. The main parameters were kept the same as suggested by the software. However, the optical parameters were changed to accommodate the study’s optical efficiency values (0.5; 0.6, and 0.7). The Schott PTR80 receiver was chosen and maintaining the other parameters default. Finally, the values related to thermal storage were set. Default values were considered as well.

The same methodology was followed for the simulations of all three absorption cycle configurations. In other words, the characteristic values of each stage such as heatsink power, inlet and outlet fluids temperature, solar multiple values optimized from the parametric analyzes, among others, were modified in the analysis of each case.

The data, monthly hourly averages, was organized in Microsoft Excel® spreadsheets in order to simultaneously evaluate the thermal load profile required in the absorption system and the thermal load provided by the solar system. In doing so, it became possible to analyze the effects of the various variables adopted, as well as the hourly interaction of energy supply and requirement that allowed the determination of the auxiliary energy fraction. The results graphic presentation and their discussion are presented in section 4.

#### 4. Results and analysis

Table 6 presents the simulation result for the thermal conditioning load required per Thermal Zone of the university complex building. This table shows the peak heating load values required by the system’s evaporator, the room temperature, and the outside temperature. The software returns the values for peak’s day and hour, thermostat temperature, and specific air humidity. These values are essential for the characterization of the load curve as well as the determination of the input parameters for the CST modeling. Zones 7, 8, and 9 (toilets on the 1<sup>st</sup>, 2<sup>nd</sup>, and 3<sup>rd</sup> floors) do not have cooling systems, consequently, they are not included in the table, despite influencing the ambient thermal load.

The sum of the thermal load demanded by the evaporator is fundamental for the definition of the generator power. The thermal load for each building is 263,572 W, so the total load for the three buildings is equal to 790,716 W. Table 7 expresses the ratio of this load to the COP values from generator thermal load. The generator thermal load values were rounded and inserted in the SAM as input data for the solar-powered air-cooling system simulation.

Table 8 provides an example for the variables parameterization results that optimize the annual energy production (solar multiple and outlet fluid temperature) and the relevant output data for each case on the double-effect system. The same methodology was applied for single- and triple-effect cases.

As expected, an increase in energy production is observed for the following cases: same solar multiple and high storage time; high efficiency, but similar solar multiple and storage time; high solar multiple and same efficiency.

Table 8 only exposes the optimal parameterization values and the output values, which are not the focus of the study's analysis. This table points out the variables quantitative aspect in each case mentioned.

The following subsection introduces the results of the load produced and demanded by the three different absorption system configurations (single-, double- and triple effect). These results are exposed through curves prepared in a spreadsheet with the average hourly loads per month. Due to the large number of cases in each configuration (9 in each), only two cases were selected for the load curves detailed discussion and graphic display.

After modeling the buildings thermal load, the study needs to understand the interaction between the thermal energy produced by the solar system and required by the cooling systems (single, double- and triple effect). For each configuration, a graphical demonstration is conducted for the interaction between the energy demand and production curves based on hourly averages for each month. The extreme cases simulated were considered for the demonstration, which are the lowest optical efficiency (0.5) and 6 hours of storage; and the best efficiency (0.7) and 10 hours of storage.

Table 6.  
Simulation results for the thermal conditioning load

Thermal Zone	Peak heating load (W)	Room temperature (°C)	Outside temperature (°C)
1	25389	22.99	32.71
2	33069	22.98	33.21
3	64552	22.98	33.43
4	76028	22.98	32.71
5	24068	22.98	32.71
6	27734	22.98	32.44
10	12729	22.98	32.44

Source: the authors.

Table 7.  
Thermal load required by the absorption cooling system generator.

Absorption cycle	COP	Generator thermal load (kW)	Value inserted in SAM (MW)
Single-effect	0.65	1.216	1.2
Double-effect	1.36	581	0.58
Triple-effect	1.80	439	0.43

Source: the authors.

Table 8.  
SAM simulation results for the double-effect cooling system

Case	Multi ple Solar	Outlet Fluid temperature (°C)	Annual net energy (kWh-t)	Annual electricity load (kWh-e)	Total reflective area (m <sup>2</sup> )
LE/06	3.0	170	1,384,527	63,172	15,180
LE/08	3.0	170	1,577,701	67,469	15,180
LE/10	3.0	170	1,719,000	72,605	15,180
ME/06	3.0	170	1,465,518	42,513	12,420
ME/08	3.0	170	1,654,163	45,853	12,420
ME/10	3.0	170	1,793,488	48,585	12,420
HE/06	3.0	180	1,496,540	36,735	11,040
HE/08	3.0	190	1,592,038	44,847	11,040
HE/10	3.0	170	1,902,196	46,752	11,040

Source: the authors.

#### 4.1.1 Results for the single effect configuration

This subsection presents the thermal load curves provided by the CST system (supply) and required by the single effect absorption refrigeration cycle (demand) generator, LE/06 and HE/10 cases.

- Single-effect configuration case LE/06

The LE/06 case has its optical efficiency of 0.5 and 6h of storage. For the single effect system, as highlighted in the methodology, the results demonstrate a greater need for thermal energy due to the lower COP values. That is, high values on the demand curves (dot lines).

As observed in January, the energy production is considerably higher than energy demand in most hours, due to the lower energy required during academic breaks. Conversely, the thermal load required from February to December is higher, demanding 50% more auxiliary energy. Therefore, a complementary energy source would be required to supply extra energy and suffice the energy deficit. July is the month with the highest demand for auxiliary energy (73.43%). In summary, the proposed configuration would supply around 40% of the complex's annual energy demand.

- Single-effect configuration case HE/10

The simulation results for the single effect system case HE/10 presented similar profiles. The required auxiliary demand achieves the lowest value in January and highest value (69%) in July in comparison to other months. This proposed case would supply an average of 44% of the annual energy demand.

The annual auxiliary energy requirement sum was 60% and 57% for the LE/06 and HE/10 configuration cases, respectively. The biggest difference from LE/06 to HE/10 case is observed in the month of May, showing an approximate decrease of 8%. However, the configuration in both cases necessitates considerable amounts of auxiliary energy.

#### 4.1.2 Results for the double-effect configuration system

This subsection addresses the thermal load curves provided by the CST system and required by the absorption refrigeration cycle generator. However, this subsection tackles the results for the double effect system configuration using the LE/06 and HE/10 cases.

- Double-effect configuration case LE/06

Figs. 2, 3 and 4 display the results referring to the double effect system case LE/06. The figures show the thermal load produced by the CST system, the load required by the air conditioning system, and the difference between the two loads, for each four-month period of the year. It is noteworthy that the demand curves (blue lines) for each month have narrowed. This behavior is a reflection of the higher COP values achieved by the double-effect system compared to the single-effect system, which implies fewer thermal energy requirements.

As observed, even in the lower efficiency case, LE/06, the entire demand curve is below the energy curve produced in January. In other words, the system is self-sufficient for that month as all the thermal energy required is supplied by the CST system. Regarding the auxiliary energy needs, February to December mostly reached values below 50%. Except for the months of June and July that have a higher requirement, achieving demand of 58% and 62%, respectively. Hence, the proposed case would produce around 77% of the complex's average annual energy demand.

- Double-effect configuration case HE/10

In the double effect configuration system case HE/10 (Figs. 5, 6 and 7), auxiliary energy is not required from January to March, August to September, November and December, as the energy requirement falls below 10% of the system. The energy demand is the highest in July, requiring 50% more auxiliary energy. The proposed high efficiency double effect configuration system would supply around 84% of the complex's average annual energy demand.

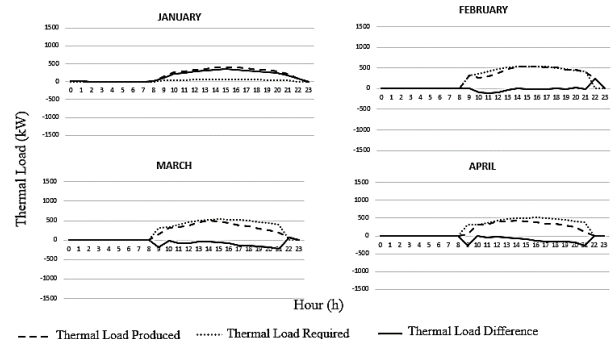


Figure 2. Thermal loads comparison, 1<sup>st</sup> quarter of the year, for the double effect configuration case LE/06.

Source: the authors.

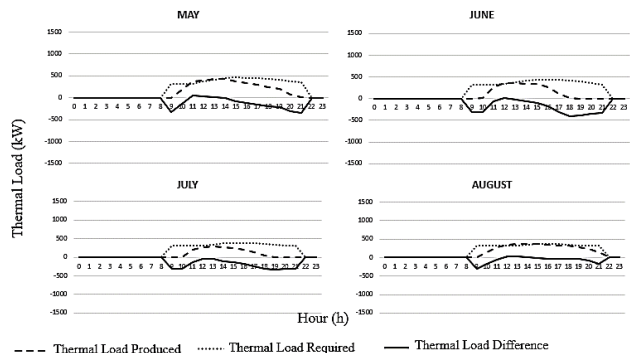


Figure 3. Thermal loads comparison, 2<sup>nd</sup> quarter of the year, for the double effect configuration case LE/06.

Source: the authors.

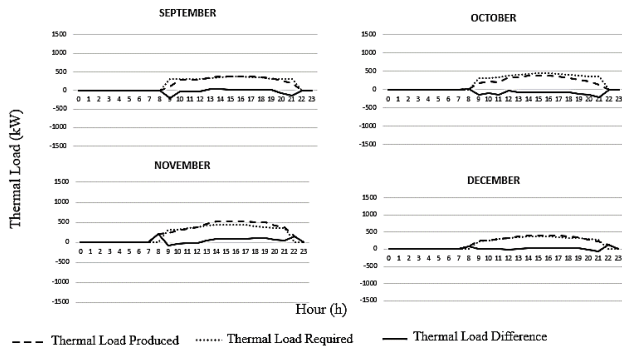


Figure 4. Thermal loads comparison, 3<sup>rd</sup> quarter of the year, for the double effect configuration case LE/06. Source: the authors.

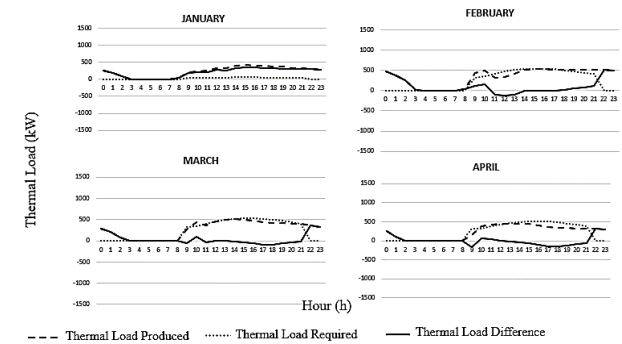


Figure 5. Thermal loads comparison, 1<sup>st</sup> quarter of the year, for the double effect configuration case HE/10. Source: the authors.

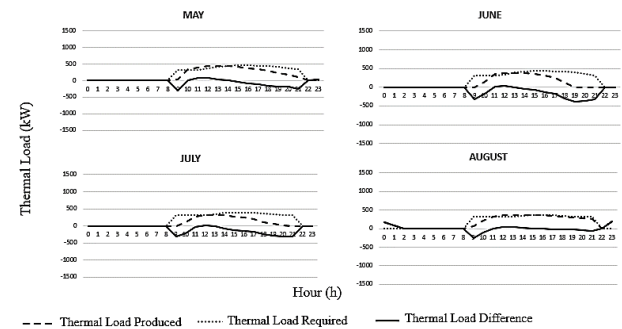


Figure 6. Thermal loads comparison, 1<sup>st</sup> quarter of the year, for the double effect configuration case HE/10. Source: the authors.

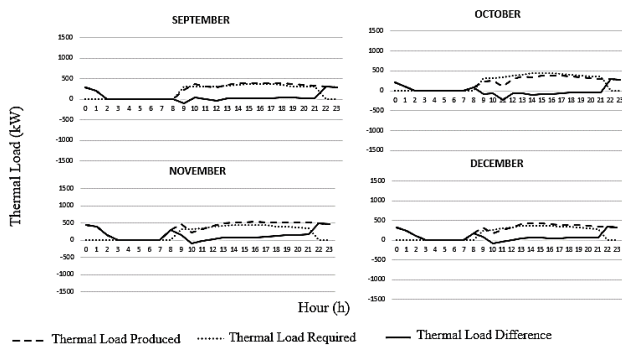


Figure 7. Thermal loads comparison, 3<sup>rd</sup> quarter of the year, for the double effect configuration case HE/10. Source: the authors.

### 4.1.3 Results for the triple-effect configuration system

This subsection presents the thermal load curves provided by the CST system and required by the triple-effect absorption cooling cycle generator. In order to compare with the systems previously analyzed, the conditions for efficiency and storage time will be presented. In other words, cases LE/06 and HE/10 with triple-effect configuration.

- Triple-effect configuration case LE/06  
For the months with good solar incidence (between November and April), the system's outputs reach satisfactory results with auxiliary energy requirements below 50%. Nevertheless, in the second quadrimester, the system needs up to 91% of additional energy as the triple-effect cooling system requires high quality heat but only receives low solar incidence in these months. So, the system works at high temperatures.
- Triple-effect configuration case HE/10  
In the simulations for the triple-effect configuration case HE/10, the energy production in January is about 6 times superior to the demand, configuring a high energy surplus. In the first four-month period of the season, the energy production is relatively significant due to the higher radiation levels, expecting only 12% of auxiliary energy. In the other months, nonetheless, the auxiliary energy requirement increases, on average, to 56%.

Table 9 shows the fractions of the auxiliary energy required in cases LE/06 and HE/10 for double and triple effect system per month.

By comparing the double effect configuration cases LE/06 and HE/10, the main difference between the two cases is noted in March, with an approximate decrease of 16%. From case AE/10 to case BE/06, there is an average 7% monthly reduction in auxiliary energy demand. Overall, both cases have rates of auxiliary energy demand significantly lower than systems with single-effect configuration (about 35%). Hence, the energy balance for double-effect configuration systems has technically sound advantages. In addition, there are many double-effect air refrigeration systems available in Brazilian, companies such as Thermax do Brasil and TUMA/BROAD commercialize double effect absorption technologies

In the triple-effect configuration systems, cases LE/06 and HE/10, the proposed case system would generate 58% of the complex's energy demand on an annual average.

By comparing both cases with double- and triple effect systems, the results show a higher demand for auxiliary energy in the triple-effect configuration. Although triple-effect systems have higher COP values than double-effect systems, they need high quality heat for operation. The simulations also demonstrated that the triple-effect systems, for both cases, require an average of 48% auxiliary energy, which indicates a 28% higher demand compared to the double effect system.

For a better analysis between energy quantity and quality in both double- and triple-effect systems, Figs. 8 and 9 proposed a combined visualization of the DNI hourly behavior, and the heat sink thermal power, for three days and in different seasons of the year. Fig. 8 shows the hourly behavior of the heat sink's thermal power and its interaction with DNI for the 1<sup>st</sup>, 2<sup>nd</sup>, and 3<sup>rd</sup> day of January. Fig. 9 demonstrates this behavior for the interval from 30 June to 2 July. The simulated case for both configurations (double and triple effect) considered the HE/10 case.

Table 9. Auxiliary energy required by cases with double effect and triple effect configuration system

Month	Double Effect		Triple-effect	
	LE/06	HE/10	LE/06	HE/10
January	0%	0%	0%	0%
February	6%	6%	7%	7%
March	24%	8%	35%	14%
April	28%	17%	62%	25%
May	37%	25%	78%	49%
June	58%	47%	89%	73%
July	62%	50%	91%	77%
August	21%	12%	69%	58%
September	11%	3%	60%	53%
October	26%	20%	65%	59%
November	3%	2%	43%	41%
December	2%	2%	47%	42%
Annual average	23%	16%	54%	42%

Source: the authors.

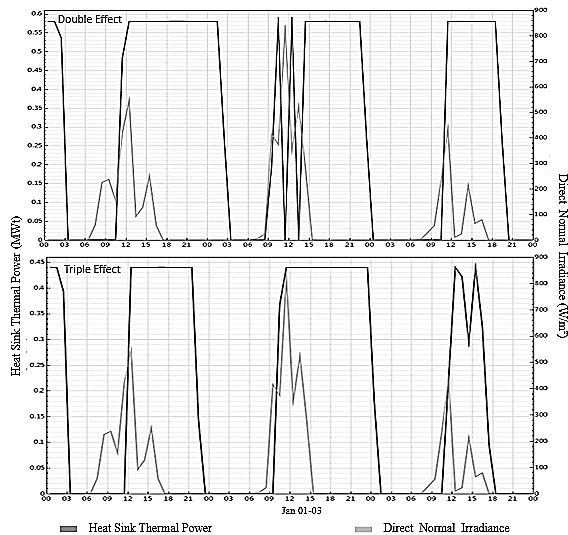


Figure 8. Thermal loads comparison between the double- and triple-effect configuration system for the 1<sup>st</sup>, 2<sup>nd</sup>, and 3<sup>rd</sup> days of January. Source: adapted from [21].

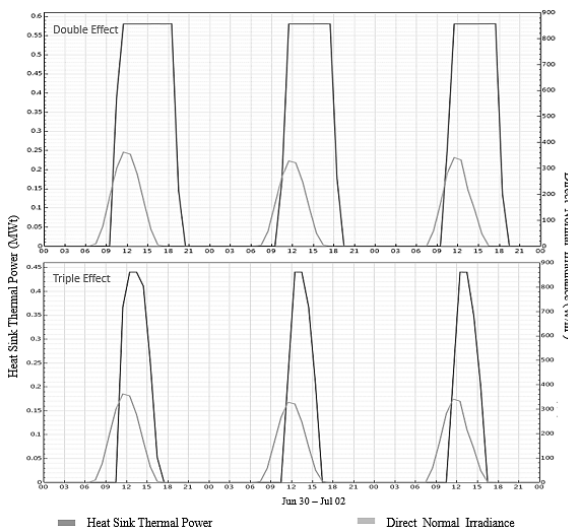


Figure 9. Thermal loads comparison between the double- and triple effect configuration system from June 30<sup>th</sup> to July 2<sup>nd</sup>. Source: adapted from [21].

The trends from Fig. 8, show that on the 1<sup>st</sup> and 3<sup>rd</sup> days of January (days with medium radiation) the double effect-system performs better and produces more energy, with longer operating time and greater stability (fewer interruptions in operation). For days with high DNI (January 2<sup>nd</sup>), the triple-effect configuration system gives the best energy production result, a consequence of the better quality (temperature) of the heat delivered to the absorption refrigeration generator. On the other hand, for months with lower radiation, the double-effect system outperforms the triple-effect configuration in terms of daily energy production, which can be seen in the wider curves throughout the day, Fig. 9.

The estimates show that although triple effect cooling systems require less energy, they need higher quality energy (heat at a higher temperature) that is directly related to the level of local direct radiation. The results indicate the double-effect system has a better local performance. However, it is worth mentioning that the simulations were conducted for a CST application in a specific site, not a universal case. For sites with better radiation levels, the triple-effect absorption cooling system can show superior results.

### 5. Conclusions

The current work investigates the techno feasibility of solar air conditioning systems in a University Complex (UFRJ) located in the city of Macaé- RJ, Brazil. The study uses a combined simulation procedure based on building thermal comfort and concentrating solar thermal (CST) technology associated with absorption refrigeration systems. The study sought to propose and test a methodological procedure applied to an alternative energy system. Furthermore, this methodology was developed to identify the best possible configuration for an air-cooling system, operating at different levels of optical efficiency, at the UFRJ-Macaé Campus.

Simulations were performed to estimate the thermal load required by the building and the energy produced by the CST system. SketchUp, OpenStudio, and EnergyPlus software was used to calculate the building's thermal load. The System Advisor Model software was used to calculate the solar field thermal energy output and simulate the system' operating with thermal storage. Data treatment, refining, and manipulation were conducted in an electronic spreadsheet in order to assess the difference between the demanded and the offered energy on an hourly basis. Then, it was possible to assess the auxiliary energy required to secure the system's safe operation. The auxiliary energy estimates also made it possible to ascertain the energy adequacy of the proposed system to the university campus. The assumption behind this application is that this system could not only have pilot plant functions for technological learning but also contribute to supply the building air conditioning demand.

SketchUP, OpenStudio and EnergyPlus software proved to be important tools for appraising the building's thermal load. They were also useful to provide the thermal load and peak temperatures for the different thermal zones of university rooms. The programs allowed appropriate modeling of the building, as well as the introduction of the



construction parameters and the ambient usage profile. Thus, enabling the determination, with proximity to reality, of the energy consumption for the building's conditioning. The simulated thermal load was 790.716 W.

SAM software enabled the simulation of the technical and energetic aspects in order to define the energy generation for the conditioning system functioning. The plant's operation considered different cases to analyze the system techno-feasibility. In all simulated cases, the same type of concentrating solar technology was used but varying optical efficiency values ( $n= 0.5; 0.6; 0.7$ ), following the data provided by scholarly literature and considering the parabolic trough under development in Macaé. Moreover, different absorption refrigerator types were used (single, double- and triple-effect), based on scholarly information and consistent with the thermodynamic analysis of these alternatives. The hours of thermal energy storage (6h, 8h and 10h) also varied in the simulations.

Satisfactory values were achieved with the simulations completed for the double effect system. This system requires an average of 20% auxiliary energy to maintain its operation, ranging from self-sufficiency in January to the peak demand in July. When compared to single and triple-effect systems, this rate differs by 35% and 28%, respectively. Therefore, although the triple-effect system presents better performance due to inferior energy requirements, it needs a heat supply at higher temperatures compared to the double effect system. In addition, because the chosen location has medium direct irradiation levels, the double-effect CST system performed better under the proposed conditions. Studies using this system applied in other locations are suggested but also considering that the introduction of a triple-effect system in places with higher direct normal radiation could return satisfactory results. In fact, in months with higher direct radiation (January to March), the triple-effect system would require less auxiliary energy.

Finally, this work contributed to the literature by providing the conditions for future applications of the air conditioning system in a public university. The pilot CST plant can be developed and improved by the teaching staff and students. Furthermore, the results presented here encourage the application of this system in other public buildings such as schools and hospitals.

## Referencias

[1] Pereira, E.B., Martins, F.R., Gonçalves, A.R., Abreu, S.L., de Costa, R.S., Lima, F.J.L., Pereira, S.V., Tiepolo, G.P., Souza, J.G. y Rüther, R., Atlas Brasileiro de Energia Solar 2<sup>da</sup> ed., INPE, São José dos Campos, Brasil, 2017.

[2] Basso, L.H., Souza, S.N.M., de Siqueira, J.A.C., Nogueira, C.E.C. and Santos, R.F., Análise de um sistema de aquecimento de água para residências rurais, utilizando energia solar. Engenharia Agrícola, 30(1), pp. 14-21, 2010.

[3] Drosou, V., Kosmopoulos, P. and Papadopoulos, A., Solar cooling system using concentrating collectors for office buildings: a case study for Greece. Renewable Energy, 97, pp. 697-708, 2016. DOI: 10.1016/j.renene.2016.06.027

[4] Soria, R., Schaeffer, R. and Szklo, A.S., Configurações para operação de plantas heliotérmicas CSP com armazenamento de calor e hibridização no Brasil. In: V Congresso Brasileiro de Energia Solar, 2014, V Congresso Brasileiro de Energia Solar, Recife, Brasil, 2014.

[5] Malagueta, D.C., Szklo, A.S., Soria, R.P., Dutra, R., Schaeffer, R. and Borba, B.S.M.C., Potential and impacts of Concentrated Solar Power (CSP) integration in the Brazilian electric power system, Renewable Energy, 68, pp. 223-235, 2014. DOI: 10.1016/j.renene.2014.01.050.

[6] Malagueta, D.C., Avaliação de alternativas para introdução da geração elétrica termossolar na matriz energética Brasileira. Tese Doutorado - UFRJ/ COPPE, Rio de Janeiro, Brasil, [em linha]. 2013. Disponível em: [http://www.ppe.ufrj.br/images/publica%C3%A7%C3%B5es/doutorado/Diego\\_Cunha\\_Malagueta.pdf](http://www.ppe.ufrj.br/images/publica%C3%A7%C3%B5es/doutorado/Diego_Cunha_Malagueta.pdf).

[7] Borba, B.S.M.C., Henrique, L.F. and Malagueta, D.C., A novel stochastic optimization model to design concentrated photovoltaic/thermal systems: a case to meet hotel energy demands compared to conventional photovoltaic system. Energy Conversion and Management, 224, art. 113383, 2020. DOI: 10.1016/j.enconman.2020.113383

[8] IEA, The Future of Cooling, IEA, Paris, Francia, [online]. 2018. Available at: <https://www.iea.org/reports/the-future-of-cooling>

[9] ANEEL, Agência Nacional de Energia Elétrica – Chamada 019/2015: Projeto Estratégico: Desenvolvimento de Tecnologia Nacional de Geração Heliotérmica de Energia Elétrica, Brasil, 2015.

[10] Schaeffer, R., Szklo, A., Lucena, A., Borba, B., Nogueira, L., Fleming, F., Troccoli, A., Harrison, M. and Boulahya, M., Energy sector vulnerability to climate change: a review. Energy, 38, pp. 1-12, 2012. DOI: 10.1016/j.energy.2011.11.056

[11] Dulac, J., Abergel, T. and Delmastro, C., IEA, Tracking Buildings, IEA, Paris, France, [online]. 2019. Available at: <https://www.iea.org/reports/tracking-buildings>

[12] Duffie, J.A. and Beckman, W.A., Solar engineering of thermal processes, 3<sup>rd</sup> Ed., John Wiley & Sons, New York, USA, 2013.

[13] Torres, R.C., Energia solar fotovoltaica como fonte alternativa de geração de energia elétrica em edificações residenciais. São Carlos, Brasil, 2012.

[14] SOLARGIS. World map of direct normal irradiation. The World Bank, Global Solar Atlas 2.0, Solargis. [online]. 2019. [date of reference December 20<sup>th</sup> of 2019]. Available at: <https://solargis.com/maps-and-gis-data/download/world>

[15] Günther, M., Joemann, M. and Csambor, S., Advanced CSP teaching materials. Chapter 5: Parabolic Trough Technology ENERMENA & DRL, 2011.

[16] Stoecker, W.F. e Jones, J.W., Refrigeração e Ar Condicionado, Editora McGraw-Hill, Brasil, 1985.

[17] Noberto, L.G. de M., Análise de um sistema de refrigeração por absorção com mistura água-brometo de Lítio. Teses de grado. Universidade Federal Do Rio Grande Do Norte, Brasil, 2018.

[18] Wang, J., Yan, R., Wang, Z., Zhang, X. and Shi, G., Thermal performance analysis of an absorption cooling system based on parabolic trough solar collectors. Energies, 11(10), art. 2679, 2018.

[19] Bellos, E. and Tzivanidis, C., Parametric analysis and optimization of a cooling system with ejector-absorption chiller powered by solar parabolic trough collectors. Energy Conversion Management, 168, pp. 329-342, 2018. DOI: 10.1016/j.enconman.2018.05.024

[20] Neto, M.V., Modelação energética de sistemas de absorção em TRNSYS. Coimbra, 2016.

[21] NREL, System Advisor Model, version 2018.11.11. National Renewable Energy Laboratory. [online]. s.d. [date of reference December 20<sup>th</sup> of 2019]. Available at: <https://sam.nrel.gov/download>

[22] Carmo, N.R.M., Desenvolvimento de Software para discretização de cilindro – parabólico. Teses de grado, UFRJ, Macaé – RJ, Brasil, 2016.

[23] Almeida, M.B., Análise de perfil de temperatura do tubo absorvedor de concentradores solares por meio de simulação computacional, Teses de grado, UFRJ, Macaé – RJ, Brasil, 2018.

[24] Santos, I.F.M., Análise numérica da condução térmica transiente para diferentes fluidos em um tubo absorvedor / Igor Ferreira Martins dos Santos. – Teses de grado, UFRJ, Macaé – RJ, Brasil, 2018.

[25] Joseph, J., Estudo de um sistema de ar condicionado com assistência solar na África do Sul. Teses de grado, Escola de Engenharia, Universidade de KwaZulu-Natal. Durban, África do Sul, 2012.

[26] Al-Zubaydi, A., Building models design and energy simulation with Google Sketchup and Openstudio, Journal of Advanced Science and Engineering Research, 3(4), pp. 318-333, 2013.

- [27] Rupp, R.F., Dimensionamento de área de janela em edificações comerciais: integração da iluminação natural com a artificial e utilização da ventilação híbrida. 2011.
- [28] Sander, L.N., Dimensionamento do Sistema de refrigeração para o bloco C., Teses de grado, Campus UFRJ Macaé / Lucas Nogueira Sander, UFRJ, Macaé, Brasil, 2017.
- [29] Alghoul, S., Rijabo, H. and Mashena, M., Energy consumption in buildings: a correlation for the influence of window to wall ratio and window orientation in Tripoli, Libya. *Journal of Building Engineering*, 11, pp. 82-86 2017. DOI: 10.1016/j.jobe.2017.04.003
- [30] Zhang, X., Yang, J., Fan, Y., Zhao, X., Yan, R., Zhao, J. and Myers, S., Experimental and analytic study of a Hybrid Solar/Biomass rural heating system. *Energy*, 190, art. 116392, 2020. DOI: 10.1016/j.energy.2019.116392
- [31] Banu, P.S.A. and Sudharsan, N.M., Review of water based vapour absorption cooling systems using thermodynamic analysis, *Renewable and Sustainable Energy Reviews*, 82, Part 3, pp. 3750-3761, 2018. DOI: 10.1016/j.rser.2017.10.092
- [32] Eisa, M.A.R., Devotta, S. and Holland, F.A., Thermodynamic design data for absorption heat pump systems operating on water-lithium bromide: Part I-Cooling, *Applied Energy*, Elsevier, 24(4), pp. 287-301, 1986. DOI: 10.1016/0890-4332(88)90039-7
- [33] Kim, J.S., Park, Y. and Lee H., Performance evaluation of absorption chiller using LiBr +H<sub>2</sub>N(CH<sub>2</sub>)<sub>2</sub>OH +H<sub>2</sub>O, LiBr +HO(CH<sub>2</sub>)<sub>3</sub>OH + H<sub>2</sub>O, and LiBr +(HOCH<sub>2</sub>CH<sub>2</sub>)<sub>2</sub>NH +H<sub>2</sub>O as working fluids. *Applied Thermal Engineering* 19, pp. 217-225, 1999. DOI: 10.1016/S1359-4311(98)00032-5
- [34] Kaita, Y., Simulation results of triple-effect absorption cycles. *International Journal of Refrigeration*. 25(7), pp. 999-1007, 2002. DOI: 10.1016/S0140-7007(01)00100-1
- [35] Silva, C.L. e Moreira, H.B.C., Avaliação energética de um sistema de refrigeração por absorção utilizando gás de aterro e gás natural. *Ciência & Engenharia*, 17(1/2), pp. 11 – 16, 2008.
- [36] Kincaid, N., Mungas, G., Kramer, N., Wagner, M. and Zhu, G., An optical performance comparison of three concentrating solar power collector designs in linear Fresnel, parabolic trough, and central receiver, *Applied Energy*, Elsevier, 231(C), pp. 1109-1121, 2018. DOI: 10.1016/j.apenergy.2018.09.153
- [37] Anapolski, J.L.P. and Indrusiak, M.L.S., Energetic synthesis of a network of heat exchangers in a soybean oil refining process. *Perspectiva*, Erechim. 39(146), pp. 27-42, 2015.
- [38] Floudas, C.A. and Grossmann, I.E., Synthesis of flexible heat exchanger networks with uncertain flowrates and temperatures. *Computers & Chemical Engineering*, 11(4), pp. 319-336, 1987. DOI: 10.1016/0098-1354(87)85014-7
- [39] Cereto, A.C., Integração energética da rede de trocadores de calor em extração por solvente para a produção de farelo branco de soja. Teses de grado, Universidade Federal do Rio Grande do Sul, Brasil, 2004.
- [40] Santos, W.S. and Jesus, W.S., A Tecnologia pinch: uma proposta para o consumo sustentável de energia. Em: VII Simpósio de Engenharia de Produção de Sergipe, 2015.
- L. de O. Alves**, is BSc. Eng. in Mechanical Engineer, in 2016 from the Federal University of Rio de Janeiro, Brazil, MSc. in Energy Planning in 2020 from the COPPE/UFRJ, Brasil, and Dr. in course with conclusion estimated to 2024. Expertise in solar projects for micro and mini scale for heat and power generation. Professor at industrial mechanical technical school.  
ORCID: 0000-0002-6474-5250
- D.C. Malagueta**, is BSc. Eng. in Mechanical Engineer from the UFRJ, Brazil, MSc. and Dr. in Energy Planning from the (PPE/COPPE). Actually is Associate Professor III in the UFRJ. With experience in energy matrix, public policies, GRID, solar energy and cogeneration. Producer of a podcast called "Energia para o Cidadão", a program designed to spread knowledge.  
ORCID: 0000-0001-8352-7462
- E.P. da Rocha**, is BSc. Eng. in Chemical Engineer from the UFRRJ, Brazil. MSc. and Dr. in Metallurgical Engineer from the UFF, Brazil. Is Associate Professor at Mechanical engineering graduation at UFRJ, Brazil. Works in the fields of heat transfer and renewable energies.  
ORCID: 0000-0002-3959-2205